224-Gbps single-photodiode PAM-4 transmission with extended transmitter bandwidth based on optical time-and-polarization interleaving

Zhang, Xiaoling; Fu, Yan; Kong, Deming; Li, Longsheng; Jia, Shi; Wei, Jin; Chen, Chen; Zhang, Chongfu; Qiu, Kun; Hu, Hao

Published in:
Optics Express

Link to article, DOI:
10.1364/OE.397130

Publication date:
2020

Document Version
Publisher's PDF, also known as Version of record

Research Article | Vol. 28, No. 14 / 6 July 2020 / Optics Express 21155
Optics EXPRESS

224-Gbps single-photodiode PAM-4 transmission with extended transmitter bandwidth based on optical time-and-polarization interleaving

XIAOLING ZHANG,[1,2] YAN FU,[2] DEMING KONG,[2] LONGSHENG LI,[2] SHI JIA,[2] JIN WEI,[1] CHEN CHEN,[3] CHONGFU ZHANG,[1] KUN QIU,[1] AND HAO HU[2,*]

[1]*School of Information and Communication Engineering, University of Electronic Science and Technology of China, Chengdu 611731, China*
[2]*DTU Fotonik, Technical University of Denmark, Kgs. Lyngby, Denmark*
[3]*School of Microelectronics and Communication Engineering, Chongqing University, Chongqing 400030, China*
[*]*huhao@fotonik.dtu.dk*

Abstract: We have proposed and demonstrated the optical time-and-polarization interleaving (OTPI) technique, which can effectively extend the transmitter bandwidth for an intensity modulation and direct detection (IM/DD) optical system. The 224-Gbit/s line-rate OTPI-PAM-4 signal is successfully transmitted over a 500-m standard single-mode fiber (SSMF) in the C band, using the transmitter with a bandwidth of 25 GHz and the receiver with a single photodiode. By using a 33%-return-to-zero (RZ) pulse train, a bit-error ratio (BER) below 7% hard-decision forward error correction (HD-FEC) threshold is achieved. BER below 20% soft-decision forward error correction (SD-FEC) threshold is also realized using a carrier suppressed return-to-zero (CSRZ) pulse train. The OTPI technique can also be used for more higher-order pulse amplitude modulation (PAM) formats, making it a promising technique for next-generation high-speed optical interconnects.

1. Introduction

Spurred by the dramatically increasing demand on data traffic in data-center interconnections, the next-generation networks are expected to support ubiquitous availability, ultra-low latency, high rate and high reliability services [1]. Thus, there exist urgent requirements to effectively achieve more than 200 Gb/s per wavelength high-speed transmission over standard single-mode fiber (SSMF). In the past few years, standardizations such as 200 GE and 400 GE schemes based on existing 100 GE low-cost and power-efficient components like digital-to-analog converter (DAC), driver, laser, analog-to-digital converter (ADC), and photodiode are widely considered as a promising technical solution to realize 200 Gb/s and 400 Gb/s short-reach transmission. To yield 200 GE and 400 GE, four and eight WDM channels are respectively employed and each wavelength is designed to convey a 50-Gb/s four-level pulse amplitude modulation (PAM-4) signal [2–4]. The new standardization pursued by the IEEE and multi-source agreement (MSA) groups updates the 400 GE proposals with four wavelength-multiplexed channels with 100 Gb/s/λ [5–8]. These proposals impose a stringent requirement on both single wavelength ultra-high bitrate transmissions and high-speed electrical/optical components to realize the desired high-speed transmissions.

Recently, a significant effort with advanced modulation formats in optical transmission system has been made to enhance the spectral efficiency, such as filter bank multi carrier (FBMC) modulation [9,10], discrete multi-tone (DMT) [11–13], quadrature amplitude modulation (QAM)

#397130 https://doi.org/10.1364/OE.397130
Journal © 2020 Received 15 May 2020; revised 19 Jun 2020; accepted 24 Jun 2020; published 1 Jul 2020

Optics EXPRESS

[14], and carrier-less amplitude phase (CAP) [15]. Usually, these advanced modulation formats require high-resolution DAC and ADC, as well as complex digital signal processing (DSP). On the other hand, although coherent detection can boost the link data rate with information carried on optical amplitude, phase, and polarization, it requires high-cost complex hardware including local oscillator, hybrid, and coherent receiver. Compared with above techniques, PAM-4 signaling based on intensity-modulation and direct-detection (IM/DD) has superior advantages in terms of low complexity, low cost and low power consumption for intra-datacenter interconnects (DCIs) applications [16,17].

However, PAM-4 might suffer from severe inter-symbol interference (ISI) introduced by the imperfect optical/electrical components with limited bandwidth. The bandwidth bottleneck in an IM/DD system mainly comes from the transmitter side, since the achievable bandwidth of receiver-side devices is usually two times higher than the bandwidth of transmitter-side devices. This bandwidth issue is the main limitation of the IM/DD systems, restricting the scaling of capacity [18,19]. Many efforts have been made to achieve a larger transmitter bandwidth. Table 1 compares the hardware requirements for typical PAM-4 based IM/DD single wavelength systems beyond 200 Gb/s. In [20], H. Mardoyan et. al. employed an Indium Phosphide DHBT selector power DAC (SP-DAC) for a 100-Gbaud PAM-4 transmission over 500-m SSMF transmissions. In [21], O. Ozolins et. al. reported a 100-Gbaud PAM-4 signal over 400-m SSMF based on a monolithically integrated distributed feedback (DFB) laser with a traveling-wave electro-absorption modulator. In [22], Kanazawa et. al. demonstrated the generation and detection of a 200-Gb/s PAM-4 using capacitively coupled silicon-organic hybrid (CC-SOH) modulator with a 3-dB EO bandwidth > 65 GHz. In [23], H. Xin et. al. reported a photonic-aided DAC based 120-Gbaud PAM-4/PAM-6 signal generation scheme using a 40-GHz mode-locked laser diode (MLLD). Most of these schemes apply large-bandwidth transmitters in order to fully utilize the available receiver bandwidth for a large overall capacity. However, utilizing a large-bandwidth DACs and modulators for a high symbol rate signal may be difficult and undesirable for short-reach applications considering the cost and the power consumption [24].

Table 1. Comparison PAM-4 hardware requirements for single wavelength 200G and above

Ref.	Key techniques	Electrical components	Modulator	Line rate (Gbps)	Distance	FEC limit
[20]	SP-DAC	High BW SP-DAC	35-GHZ MZM	200	0.5-km SMF	3.8e-3
[21]	100-GHz DFB-TWEAM	High BW PPG (Analog Mux)	100-GHz DFB-TWEAM	200	0.4-km SMF	2e-2
[22]	>65-GHz CC-SOHMZM	Keysight M8194A (BW 50 GHz)	>65-GHz CC-SOHMZM	200	B2B	1e-2
[23]	PA-DAC 40-GHz MLLD	Keysight M8195A (BW 25 GHz)	Multiple MZMs	240	B2B	3.8e-3
This work	28-GHz OTPI	Keysight M8195A (BW 25 GHz)	Multiple MZMs	224	0.5-km SMF	3.8e-3

In this paper, we propose an optical time-and-polarization interleaving (OTPI) technique to equivalently extend the transmitter bandwidth using only conventional components. Based on the OTPI technique, 56-GHz analog bandwidth is achieved to generate 112-Gbaud PAM-4 signal using two 25-GHz DACs and two 25-GHz MZMs in the transmitter. Pre-emphasis technique is also used to mitigate the bandwidth limitation of the DACs and the MZMs. Compared to the Ref. [23] using a 40-GHz MLLD for the pulse generation, a continuous-wave (CW) laser

Optics EXPRESS

and a MZM are used to generate 33% return-to-zero (RZ) or 67% carrier-suppressed return-to-zero (CSRZ) pulses to carry the data, making our scheme fully based on widely available conventional components. Since the generated pulses have a high duty cycle, simple optical time-interleaving will introduce strong overlap between the neighboring data pulses, resulting in unstable interference. The OTPI technique can effectively avoid the interference between the neighboring data pulses since these neighboring data pulses have orthogonal polarizations. Compared to traditional time interleaving or polarization interleaving, the generated OTPI signal is received by a single photodiode (PD) without any de-interleaving devices, making the receiver very simple and exactly same as a conventional direct-detection receiver. Compared to the scheme using a single high-bandwidth DAC and a high-bandwidth MZM, the strict bandwidth requirement in the transmitter can be relieved and device nonlinearity can be effectively mitigated, resulting in much simplified DSP and reduced latency at receiver side. The main cost of the OTPI technique is the increased hardware complexity, since two DACs and three MZMs are needed in the transmitter. However, the hardware complexity could be relieved by the potential photonic integration, since all the needed components could be potentially integrated on a silicon photonic or InP platform [25–27].

In the experiment, we experimentally demonstrated 224-Gbps OTPI-PAM-4 signal transmission over a 500-m SSMF using 33%-RZ pulses with a BER below 7% hard-decision forward error correction (HD-FEC) threshold of 3.8×10^{-3} and using CSRZ pulses with a bit error ratio (BER) below 20% soft-decision forward error correction (SD-FEC) threshold of 2.7×10^{-2}, respectively. The OTPI technique also has potential for advanced IM/DD modulation with higher-order PAM formats to achieve higher capacity, and it's also compatible with advanced coding scheme, such as trellis-coded modulation (TCM) coding [28].

2. Proposed OTPI technique

Figure 1 illustrates the operating principle of the OTPI technique. Firstly, a continuous-wave (CW) laser source is modulated by a radio frequency (RF) signal to generate either optical RZ or CSRZ pulses with a repetition rate of $f_{clk} = Fs$. With the Mach-Zehnder electrical-to-optical (E/O) modulator biased at transmission, quadrature and null point, 33%-RZ, 50%-RZ and 67%-CSRZ pulses can be generated with the RF frequency of Fs or $Fs/2$. The generated RZ or CSRZ pulses are divided into two branches, individually modulated with a PAM-4 signal with a symbol rate of Fs by two E/O modulators (E/O 2 and E/O 3) driven by two digital-to-analog converters (DACs). The relative delay of the two branches are fine tuned in order to achieve the interleaving in time, i.e. the peak of the data pulses in one branch aligned to the null of the data pulses in the other branch, as shown in the inset of Fig. 1. The two branches are then combined by a polarization-beam combiner (PBC) with orthogonal polarizations, which can significantly reduce the interference between the two branches and have excellent stabilities. Thus, an OTPI-PAM-4 signal is generated with an overall symbol rate of $2Fs$, which is then transmitted through a SSMF. After the transmission, the received optical signal is directly detected by a single-end photodetector (PD). Note that the OTPI technique is different from the traditional optical time-division multiplexing (OTDM) scheme [29–32], which typically requires an OTDM de-multiplexer and multiple receivers.

It should be noted that the CW laser source, optical RZ/CSRZ pulse carver, E/O modulators, delay lines and PBC could be potentially integrated on a single chip with the development of the silicon photonic or InP based fabrication and manufacture. Experimental demonstrations of integrated InP modulators with RF drivers and lasers have been reported in [33,34], where the integrated optical/electrical devices at a single-chip enable a small footprint and miniaturization system for datacenter interconnect. The integrated system would have excellent stability since the environmental factors such as the vibration and temperature fluctuation can be effectively avoided.

Optics EXPRESS

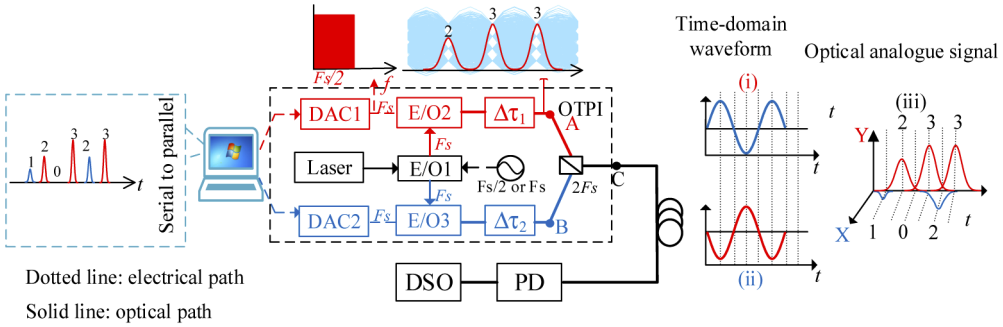

Fig. 1. Operation principle of the proposed OTPI technique.

3. Experimental setup

Figure 2 shows the experimental setup of 224-Gbps PAM-4 signal transmission using the proposed OTPI technique. At the transmitter side, a CW light with a center wavelength of 1550 nm and output power of 13.5 dBm is fed into an MZM driven by a 28-GHz RF signal. The MZM1 is biased at null point to generate optical CSRZ pulses or at peak point to generate the 33% optical RZ pulses, respectively. The pulses are then amplified to 24 dBm by an Erbium-doped fiber amplifier (EDFA) and filtered by an optical band-pass filter (OBPF) with a passband of 1 nm and insertion loss of 2.8 dB is used to remove the amplified spontaneous emission (ASE) noise induced by this EDFA. The generated pulses pass through a polarization controller and a polarizer to align the polarization, and then equally divided into two branches by a 50/50 polarization-maintaining optical coupler (PM-OC) and launched into two MZMs (MZM2 and MZM3), which are biased at the quadrature point. Each modulator is driven by a 56-Gbaud PAM-4 signal, where the random bit sequence with a length of 2^{17} is used.

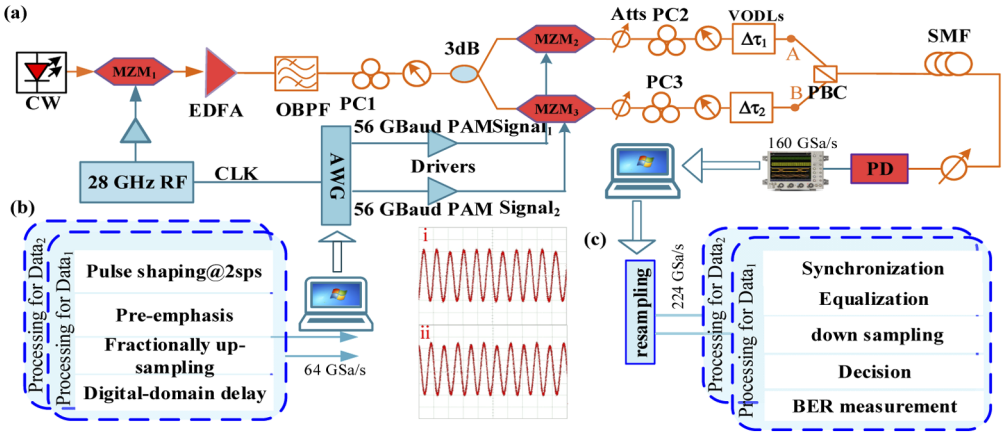

Fig. 2. Experimental setup of the proposed OTPI-enabled system.

The digital signal is upsampled to 2 sample per symbol and then Nyquist shaped with a roll-off factor of 0.01. Due to the limited bandwidth of the transmitter components, a 64-tap pre-emphasis filter is applied to compensate distortion from the transmitter. Then the signal is resampled to 64 GSa/s and generated by an arbitrary waveform generator (AWG, Keysight M8195A). The MZM1 MZM2 and MZM3 have insertion losses of 7dB, 6.5 dB and 8dB, respectively. Variable optical attenuators (VOAs) are used to equalize the optical power at the output of the MZM2 and MZM3.

Optics EXPRESS

Since the pigtail of the MZMs and the VOAs are non-PM, two polarization controllers (PC2 and PC3) and two polarizers are used to align the signal input polarization with the slow axis of the polarization-maintaining variable optical delay line (VODL). The variable optical delay lines (VODLs) introduce a relative delay of 8.93 ps between the two branches for interleaving the two 56-Gbaud PAM-4 signals in the time domain. Then two branch outputs are combined by a polarization beam combiner (PBC) with orthogonal polarizations (X- and Y-polarization) to achieve the polarization interleaved 112-Gbaud PAM-4 signal. Insets (i) and (ii) of Fig. 2 show the time interleaved RZ pulses for the two branches with peak power aligned in time to null power for each other, measured by an optical sampling oscilloscope (Keysight, 86100A) with a bandwidth of 70 GHz. Note that the eye diagrams seem like an NRZ signal due to the limited bandwidth of the sampling oscilloscope. It is worthwhile to note that the RF generator and the AWG are synchronized.

The combined 224 Gbit/s OTPI-PAM-4 signal is amplified before launching into the SSMF (CD of 17 ps/nm/km and attenuation of 0.2 dB/km). The total span loss including connection losses is 2.2 dB. At the receiver side, a VOA is placed before the single-ended PIN photodiode (XPDV3120R) to evaluate the performance versus the received optical power. The photodetected signal is digitalized by a real-time digital storage oscilloscope (Keysight DSOZ634A) with 63-GHz bandwidth and 160-GSa/s sampling rate. Finally, the received electrical signal is processed offline. The offline DSP procedure is presented in Fig. 2(c), including resampling, synchronization, digital matched filtering, and T/2-spaced second-order Volterra equalization. We use two independent equalizers for the two 56-Gbaud PAM-4 tributaries to mitigate the timing error of the pulses due to imperfect time delays applied in the transmitter. Two training sequences are used independently for the two tributaries. Finally, PAM de-mapping and BER counting are performed.

4. Experimental results

4.1. 224-Gbps OTPI-PAM-4 transmission using CSRZ pulses

We use a 112-GBaud PAM-2 signal to show the time and polarization alignment required by the OTPI technique. The eye diagrams and optical signal spectra of the two 56-Gbaud tributaries (A and B) and the 112-Gbaud OTPI signal carried by CSRZ pulses are illustrated in Fig. 3. We separately optimized individual tributary by turning off the other tributary to observe a clear and open eye diagram. Then, we adjust the VODL to make the two tributaries interleaved in time, i.e. the peak power of one tributary is aligned in time to the null power of the other tributary. We use the VOA in each branch to equalize the power for the two tributaries. Since the MZM1 is biased at null point, the optical carrier are suppressed as show in the Fig. 3(b). The CSRZ pulses have a duty cycle of 67%, thus the extinction ratio of the combined 112-GBaud PAM-2 signal is low due to the strong overlap in time between neighboring data pulses, as show in the in Fig. 3(a). As a benefit of the orthogonal polarizations between the neighboring pulses, unstable interference is avoided although there is the strong overlap between the neighboring pulses after the time interleaving.

Figure 4 shows the experimental results of the 224-Gbps OTPI-PAM-4 signal using CSRZ pulses in the back-to-back (B2B) case and after 500-m transmission. The BER results show negligible performance difference between the two tributaries before and after transmission. The receiver sensitivities for the two tributaries (A and B) with the BER at the 20% SD-FEC threshold of 2.7×10^{-2} are 5.3 dBm, 5.6 dBm for the B2B case, and 5.8 dBm, 5.8 dBm after 500-m transmission, respectively. In short, the 224 Gbps OTPI-PAM-4 is successfully transmitted over a 500-m SSMF in C band with a net rate of 186.7 Gbit/s after subtracting the overhead. Insets (a) and (b) show the signal levels, eye diagram and histogram of the recovered signal at ROP of 7.5 dBm for the tributary A before and after the transmission.

Optics EXPRESS

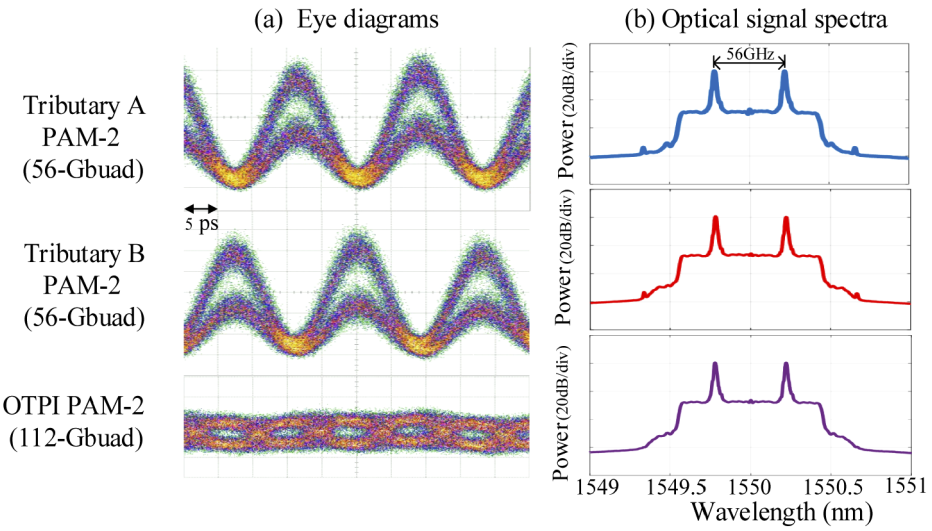

Fig. 3. OTPI-PAM-2 signal using CSRZ pulses eye diagram (a) and the optical spectra (b) of tributary A, tributary B and combined signal using the OTPI technique.

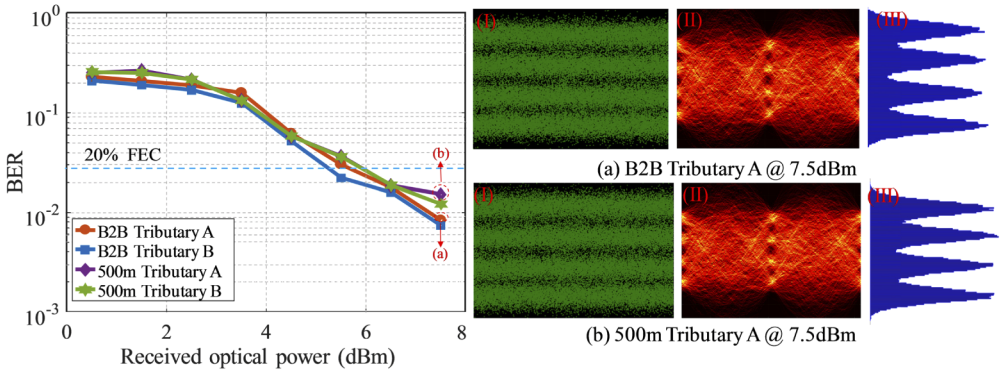

Fig. 4. Performance evaluation of CSRZ-OTPI 224Gbps PAM-4 signal in B2B configuration and after 500 m.

There are mainly two reasons for the relatively high BER even in the B2B case when using the CSRZ pulses to carry the OTPI signal. One is too high pulse duty cycle of 67% for the CSRZ pulses, which leads to the strong overlap in time after the time and polarization interleaving and consequently a low extinction ratio for the generated OTPI signal. The pulse duty cycle of 50% or below can effectively improve the extinction ratio of the OTPI signal and we achieved better BER performance by using the 33%-RZ pulses as shown in the following. The other reason is that the PBC used in the experiment to combine the polarization interleaved signal has a limited polarization extinction ratio of 25 dB, which will limit the signal to noise ratio of the generated OTPI signal. We simulate the impact of the polarization extinction ratio of the PBC on the BER performance of the OTPI signal in the B2B case, as shown in Fig. 5. The simulation results show that the polarization extinction ratio of the PBC plays a vital role on the BER performance and the BER can be significantly improved if the PBC can have a higher extinction ratio. When the polarization extinction ratio of the PBC is increased from 25 dB to 30 dB, the BER can be improved by an order of magnitude. The simulation results show much better BER performance

Optics EXPRESS

than that achieved in the experiment, which is attributed to the non-ideal implementation in the experiment.

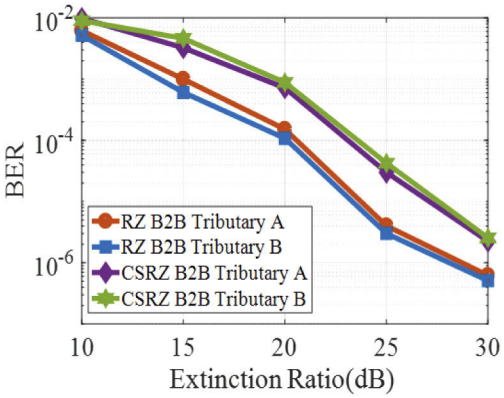

Fig. 5. Simulated BER performance for the different polarization extinction ratios of the PBC used to combine the polarization interleaved signal.

4.2. *224-Gbps OTPI-PAM-4 transmission using 33%-RZ pulses*

We further investigate the OTPI-PAM-4 transmission performance using the 33%-RZ pulses. The eye diagrams of the two 56-Gbaud tributaries (A and B) and the 112-Gbaud OTPI-PAM-2 signal are illustrated in Fig. 6(a) to demonstrate the timing alignment. The corresponding optical signal spectra are shown in Fig. 6(b). Figure 7 shows the BER performance as a function of the ROP for the 112-Gbaud OTPI-PAM-4 signal using 33%-RZ pulses before and after transmission. The BER performances after transmission is slightly worse than those in the B2B case, mainly due to chromatic dispersion from the 500-m SSMF. The signal levels, eye diagrams and histograms of the recovered signal of the tributary B with 7.5-dBm ROP before and after transmission are also shown in Fig. 7. The BER below 3.8×10^{-3} (7%-OH HD-FEC limit) can be achieved with 5.5-dBm ROP in the B2B case and with 6.5-dBm ROP after the 500-m transmission. The net

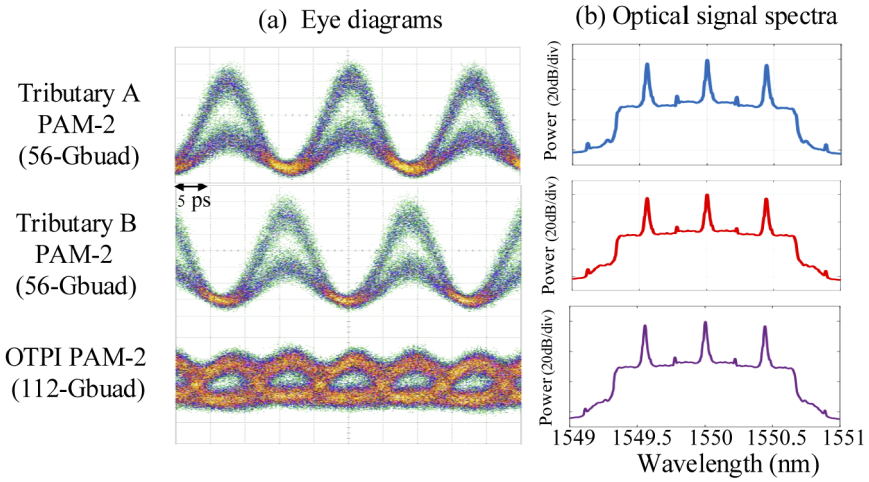

Fig. 6. (a) RZ-OTPI OOK eye diagram of tributaries A, tributaries B and final output; (b) Optical spectra of RZ-OTPI OOK signal, resolution: 20dB/grid.

Optics EXPRESS

rate of the OTPI-PAM-4 signal using the 33%-RZ pulses is 209.3 Gbit/s after subtracting the overhead. The results show that the OTPI-PAM-4 transmission using 33%-RZ pulses has better performance than using 67% duty cycle CSRZ pulses, since the lower duty cycle of the data pulses can lead to less overlap in time for the neighboring data pulses and consequently higher extinction ratio for the generated OTPI signal. According to the simulation results in the Fig. 5, the BER performance can be significantly improved if the PBC used in the experiment has a higher polarization extinction ratio. Actually, a PBC with a polarization extinction ratio of 30 dB or even higher is commercially available. The 500-m transmission distance in the experiment is limited by the optical fiber chromatic dispersion, which can be mitigated by using dispersion compensating fiber, VSB filtering or THP precoding at the transmitter side [35–37], and longer transmission distance can be achieved.

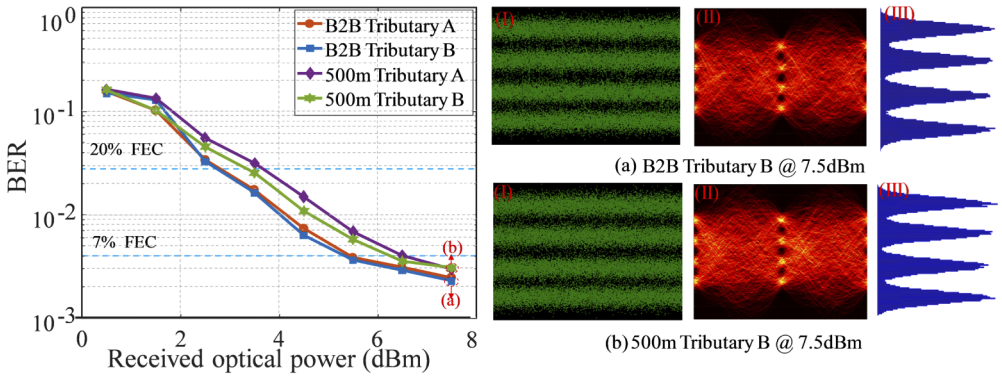

Fig. 7. Performance evaluation of 224Gbps OTPI-PAM-4 signal using 33%-RZ pulse for the B2B case and after 500-m transmission.

5. Conclusions

In this paper, we have proposed and demonstrated the OTPI technique to extend the transmitter bandwidth. The OTPI technique can effectively avoid the nonlinear distortions caused by the limited transmitter bandwidth. In addition, all the components used in the OTPI technique, such as E/O modulators, delay lines and PBC, could potentially be integrated on a silicon photonic or InP chip with a compact footprint. We measured the transmission performance of the 224 Gbit/s OTPI-PAM-4 signal using either 67%-CSRZ pulses or 33%-RZ pulses. The BER below the SD-FEC limit with 20% overhead and below the HD-FEC limit with 7% overhead after the 500-m transmission can be achieved using the 67%-CSRZ pulses and 33%-RZ pulses, respectively. The proposed OTPI technique is the key to enable the data rate >200 Gbit/s per lane PAM-4 transmission by using the DACs and modulators with a limited bandwidth. Furthermore, the OTPI technique is compatible to higher-order PAM modulation formats, making it a promising technique for next-generation high-speed optical interconnects.

Funding

Villum Young Investigator program (2MAC); Villum Fonden (15401); China Scholarship Council (201806070250); National Key Research and Development Program of China (2018YFB1801302); Colleges Innovation Project of Guangdong (2018KCXTD033); Zhongshan Social Public Welfare Science and Technology (2019B2007); Zhongshan Innovative Research Team Program (180809162197886); Research Project for Talent of UESTC Zhongshan Institute (418YKQN07).

Optics EXPRESS

Disclosures

The authors declare no conflicts of interest.

References

1. NGMN 5G White Paper, Jul. 2015, [online] Available: https://www.ngmn.org/uploads/media/NGMN_5G_White_Paper_V1_0.pdf.
2. IEEE P802.3bs 400 Gb/s Ethernet Task Force, 2018. http://www.ieee802.org/3/bs/.
3. "Ethernet alliance roadmap," http://www.ethernetalliance.org/roadmap.
4. J. L. Wei, Q. Cheng, R. V. Penty, I. H. White, and D. G. Cunningham, "400 Gigabit Ethernet using advanced modulation formats: Performance, complexity, and power dissipation," IEEE Commun. Mag. **53**(2), 182–189 (2015).
5. "IEEE P802.3bs 400GbE Task Force Public Area" (Mar. 2015), retrieved http://www.ieee802.org/3/bs/public/15_03/index.shtml.
6. "100GLambda MSA," http://100glambda.com, 2018.
7. K. Zhong, X. Zhou, T. Gui, L. Tao, Y. Gao, W. Chen, J. Man, L. Zeng, A. P. T. Lau, and C. Lu, "Experimental study of PAM-4, CAP-16, and DMT for 100 Gb/s short reach optical transmission systems," Opt. Express **23**(2), 1176–1189 (2015).
8. E. El-Fiky, M. Osman, A. Samani, C. Gamache, M. H. Ayliffe, J. Li, M. Jacques, Y. Wang, A. Kumar, and D. V. Plant, "First demonstration of a 400 Gb/s 4λ CWDM TOSA for datacenter optical interconnects," Opt. Express **26**(16), 19742–19749 (2018).
9. H. N. Parajuli, H. Shams, L. G. Gonzalez, E. Udvary, C. Renaud, and J. Mitchell, "Experimental demonstration of multi-Gbps multi sub-bands FBMC transmission in mm-wave radio over a fiber system," Opt. Express **26**(6), 7306–7312 (2018).
10. T. H. Nguyen, L. Bramerie, M. Gay, M. K. Lagha, C. Peucheret, R. Gerzaguet, S. P. Gorza, J. Louveaux, and F. Horlin, "Experimental demonstration of the tradeoff between chromatic dispersion and phase noise compensation in optical FBMC/OQAM communication systems," J. Lightwave Technol. **37**(17), 4340–4348 (2019).
11. X. Chen, Y. Chen, M. Tang, J. Cui, S. Fu, L. Xia, and D. Liu, "Optimally partitioned precoding assisted hybrid constellation entropy loading for SSB-DMT systems," in *Optical Fiber Communication Conference (OFC) 2019*, OSA Technical Digest (Optical Society of America, 2019), paper M1H.4.
12. J. L. Wei, C. Sanchez, and E. Giacoumidis, "Fair comparison of complexity between a multi-band CAP and DMT for data center interconnects," Opt. Lett. **42**(19), 3860–3863 (2017).
13. X. Chen, C. Antonelli, S. Chandrasekhar, G. Raybon, A. Mecozzi, M. Shtaif, and P. Winzer, "Kramers–Kronig receivers for 100-km datacenter interconnects," J. Lightwave Technol. **36**(1), 79–89 (2018).
14. Z. Li, M. S. Erkılınç, K. Shi, E. Sillekens, L. Galdino, T. H. Xu, B. C. Thomsen, P. Bayvel, and R. I. Killey, "Spectrally efficient 168 Gb/s/λ WDM 64-QAM single-sideband Nyquist-subcarrier modulation with Kramers–Kronig direct-detection receivers," J. Lightwave Technol. **36**(6), 1340–1346 (2018).
15. J. L. Wei, N. Eiselt, C. Sanchez, R. Y. Du, and H. Griesser, "56 Gb/s multi-band CAP for data center interconnects up to an 80 km SMF," Opt. Lett. **41**(17), 4122–4125 (2016).
16. M. Y. Zhu, J. Zhang, X. W. Yi, H. Ying, X. Li, M. Luo, Y. X. Song, X. T. Huang, and K. Qiu, "Optical single side-band Nyquist PAM-4 transmission using dual-drive MZM modulation and direct detection," Opt. Express **26**(6), 6629–6638 (2018).
17. C. Antonelli, A. Mecozzi, and M. Shtaif, "Kramers–Kronig PAM transceiver and two-sided polarization-multiplexed Kramers–Kronig transceiver," J. Lightwave Technol. **36**(2), 468–475 (2018).
18. J. M. Estarán, S. Almonacil, R. R. Müller, H. Mardoyan, P. Jenneve, K. Benyahya, C. Simonneau, S. Bigo, J. Renaudier, and G. Charlet, "Sub-Baudrate Sampling at DAC and ADC: toward 200G per lane IM/DD systems," J. Lightwave Technol. **37**(6), 1536–1542 (2019).
19. X. D. Pang, O. Ozolins, R. Lin, L. Zhang, A. Udalcovs, L. Xue, R. Schatz, U. Westergren, S. Xiao, W. S. Hu, G. Jacobsen, S. Popov, and J. J. Chen, "200 Gbps/lane IM/DD technologies for short reach optical interconnects," J. Lightwave Technol. **38**(2), 492–503 (2020).
20. H. Mardoyan, M. A. Mestre, J. M. Estarán, F. Jorge, F. Blache, P. Angelini, A. Konczykowska, M. Riet, V. Nodjiadjim, J. Y. Dupuy, and S. Bigo, "84-, 100-, and 107-GBd PAM-4 intensity modulation direct-detection transceiver for datacenter interconnects," J. Lightwave Technol. **35**(6), 1253–1259 (2017).
21. O. Ozolins, X. D. Pang, A. Udalcovs, R. Schatz, U. Westergren, J. R. Navarro, A. Kakkar, F. Nordwall, K. M. Engenhardt, J. J. Chen, S. Popov, and G. Jacobsen, "100 Gbaud 4-PAM link for high speed optical interconnects," in *Proc. Eur. Conf. Opt. Commun.*, Gothenburg, Sweden, 2017, Paper P2.SC5.6.
22. S. Ummethala, J. N. Kemal, M. Lauermann, A. S. Alam, H. Zwickel, T. Harter, Y. Kutuvantavida, L. Hahn, S. H. Nandam, D. L. Elder, L. R. Dalton, W. Freude, S. Randel, and C. Koos, "Capacitively coupled silicon-organic hybrid modulator for 200 Gbit/s PAM-4 signaling," in *Proc. Conf. Lasers Electro-Opt.*, San Jose, CA, USA, 2019, Paper JTh5B.2.
23. H. Xin, D. Kong, K. Zhang, S. Jia, X. Zhang, W. Hu, and H. Hu, "120 GBaud PAM-4/PAM-6 generation and detection by photonic aided digital-to-analog converter and linear equalization," J. Lightwave Technol. **38**(8), 2226–2230 (2020).

Optics EXPRESS

24. O. V. Sinkin, A. V. Turukhin, Y. Sun, H. G. Batshon, M. V. Mazurczyk, C. R. Davidson, J.-X. Cai, W. W. Patterson, M. A. Bolshtyansky, D. G. Foursa, and A. N. Pilipetskii, "SDM for Power-Efficient Undersea Transmission," J. Lightwave Technol. **36**(2), 361–371 (2018).
25. P. Dong, X. Liu, S. Chandrasekhar, L. Buhl, R. Aroca, and Y.-K. Chen, "Monolithic silicon photonic integrated circuits for compact 100+ Gb/s coherent optical receivers and transmitters," IEEE J. Sel. Top. Quantum Electron. **20**(4), 150–157 (2014).
26. D. Kong, H. Xin, K. Kim, Y. Liu, L. K. Oxenløwe, P. Dong, and H. Hu, "Intra-datacenter interconnects with a serialized silicon optical frequency comb modulator," J. Light. Technol. Early Access, (2020).
27. P. Evans, M. Fisher, R. Malendevich, A. James, P. Studenkov, G. Goldfarb, T. Vallaitis, M. Kato, P. Samra, S. Corzine, E. Strzelecka, R. Salvatore, F. Sedgwick, M. Kuntz, V. Lal, D. Lambert, A. Dentai, D. Pavinski, J. Zhang, B. Behnia, J. Bostak, V. Dominic, A. Nilsson, B. Taylor, J. Rahn, S. Sanders, H. Sun, K. -. Wu, J. Pleumeekers, R. Muthiah, M. Missey, R. Schneider, J. Stewart, M. Reffle, T. Butrie, R. Nagarajan, C. Joyner, M. Ziari, F. Kish, and D. Welch, "Multi-channel coherent PM-QPSK InP transmitter photonic integrated circuit (PIC) operating at 112 gb/s per wavelength," in *Optical Fiber Communication Conference (OFC) 2011*, OSA Technical Digest (Optical Society of America, 2011), paper PDPC7.
28. Y. Fu, D. Kong, M. Bi, H. Xin, S. Jia, K. Zhang, W. Hu, and H. Hu, "Computationally efficient 104 Gb/s PWL-Volterra equalized 2D-TCM-PAM8 in dispersion unmanaged DML-DD system," Opt. Express **28**(5), 7070–7079 (2020).
29. H. Yamazaki, A. Sano, M. Nagatani, and Y. Miyamoto, "Single-carrier 1-Tb/s PDM-16QAM transmission using high-speed InP MUX-DACs and an integrated OTDM modulator," Opt. Express **23**(10), 12866–12873 (2015).
30. T. Hirooka, R. Hirata, J. Wang, M. Yoshida, and M. Nakazawa, "Single-channel 10.2 Tbit/s (2.56 Tbaud) optical Nyquist pulse transmission over 300 km," Opt. Express **26**(21), 27221–27236 (2018).
31. H. Hu, D. Kong, E. Palushani, J. D. Andersen, A. Rasmussen, B. M. Sorensen, M. Galili, H. C. H. Mulvad, K. J. Larsen, S. Forchhammer, P. Jeppesen, and L. K. Oxenlowe, "1.28 Tbaud Nyquist signal transmission using time-domain optical Fourier transformation based receiver," in *CLEO:2013*, OSA Technical Digest (online) (Optical Society of America, 2013), paper CTh5D.5.
32. H. Hu, H. C. H. Mulvad, M. Galili, E. Palushani, J. Xu, A. T. Clausen, L. K. Oxenlowe, and P. Jeppesen, "Polarization-insensitive 640Gb/s demultiplexing based on four wave mixing in a polarization-maintaining fibre loop," J. Lightwave Technol. **28**(12), 1789–1795 (2010).
33. T. Tatsumi, N. Itabashi, T. Ikagawa, N. Kono, M. Seki, K. Tanaka, K. Yamaji, Y. Fujimura, K. Uesaka, and T. Nakabayashi, "A compact low-power 224-Gb/s DP-16QAM modulator module with InP-based modulator and linear driver ICs," in *Proc. OFC 2014*, 9–13 Mar. 2014), Tu3H.5.
34. S. Chandrasekhar, X. Liu, P. J. Winzer, J. Simsarian, and R. Griffin, "Compact all-InP laser-vector-modulator for generation and transmission of 100-Gb/s PDM-QPSK and 200-Gb/s PDM-16-QAM," J. Lightwave Technol. **32**(4), 736–742 (2014).
35. X. Chen, S. Chandrasekhar, J. Cho, and P. Winzer, "Single-Wavelength and Single-Photodiode Entropy-Loaded 554-Gb/s Transmission over 22-km SMF," in *Optical Fiber Communication Conference Postdeadline Papers 2019*, (Optical Society of America, 2019), paper Th4B.5.
36. F. Bao, Y. Ding, T. Morioka, L. K. Oxenløwe, and H. Hu, "100 Gb/s SDM-PON using polarization-diversity silicon micro-ring resonator enhanced DML," J. Lightwave Technol. **36**(22), 5091–5095 (2018).
37. H. Xin, K. Zhang, D. Kong, Q. Zhuge, Y. Fu, S. Jia, W. Hu, and H. Hu, "Nonlinear Tomlinson-Harashima precoding for direct-detected double sideband PAM-4 transmission without dispersion compensation," Opt. Express **27**(14), 19156–19167 (2019).